

Article

Ginsenoside Re Ameliorates Cardiac Hypertrophy by Regulating CaSR-Mediated Signaling Pathway

Panpan Chen^{1,2,3}, Mubo Liu^{1,2,3,4}, Hong Xiao^{1,2,4}, Ting Luo^{1,2,4}, Hong Ling^{1,2,4}, Xiaoyan Chen⁵, Zongli Li⁴, Shangfu Xu^{1,2}, Zheng Li^{1,2,4} and Jiang Deng^{1,2,4,*}

¹ Key Laboratory of Basic Pharmacology of Ministry of Education, Joint International Research Laboratory of Ethnomedicine of Ministry of Education, Zunyi Medical University, Zunyi 563000, China

² Key Laboratory of Basic Pharmacology of Guizhou Province, Zunyi Medical University, Zunyi 563000, China.

³ The Affiliated Aerospace Hospital of Zunyi Medical University, Guizhou Aerospace Hospital, Zunyi 563000, China

⁴ Department of Pharmacology, School of Pharmacy, Zunyi Medical University, Zunyi 563000, China

⁵ Department of Pathophysiology, Zunyi Medical University, Zunyi 563000, China

* Correspondence: dengjiang1225@sina.com; Tel.: +86-851-2864-3411; Fax: +86-851-2864-2406

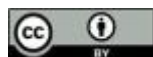
Received: 31 August 2024; Revised: 17 September 2024; Accepted: 19 September 2024; Published: 5 March 2025

Abstract: Cardiac hypertrophy is a compensatory response to pathological stimuli. Recent studies have suggested that calcium-sensing receptor (CaSR) plays an important role in the development of cardiac hypertrophy. Ginsenoside Re (Re) is a monoconstituent of the ginseng plant. Many studies have shown that Re has various beneficial pharmacological effects on the cardiovascular system. It remains uncertain if Re has an anti-cardiac hypertrophic effect through the modulation of the CaSR-mediated signaling pathway. In this research, we employed a rat model of cardiac hypertrophy to investigate the relationship between Re and CaSR. Significant reductions in blood pressure, left ventricle hypertrophic indexes, cross-sectional area of cardiomyocytes, and levels of the β -myosin heavy chain and atrial natriuretic peptide were observed in spontaneously hypertensive rats (SHR) after Re administration. In addition, Re improved cardiac structure and function in SHR. Furthermore, Re inhibited CaSR, calcineurin (CaN), nuclear factor of activated T cells 3 (NFAT3), phosphorylated zinc finger transcription factor 4 (p-GATA4), protein kinase C- β (PKC- β), rapidly accelerated fibrosarcoma-1 (Raf-1), and phosphorylated extracellular signal-regulated kinase 1/2 (p-ERK1/2). It also increased the expression of p-NFAT3 and mitogen-activated protein kinase phosphatase-1 (MKP-1). These findings suggest that Re has beneficial effects on cardiac hypertrophy in SHR. The mechanisms underlying these effects are the regulation of the PKC-MAPK axis and the CaSR-mediated signaling pathway.

Keywords: calcium-sensing receptor; ginsenoside Re; spontaneously hypertensive rats; cardiac hypertrophy; hypertension

1. Introduction

Cardiac hypertrophy is an adaptive pathophysiological event that responds to increased peripheral resistance and blood pressure. It has been linked to cardiomyocyte enlargement, increased protein synthesis, interstitial collagen deposition, sarcomere structure reorganization, and fetal gene program activation [1–9]. Although cardiac hypertrophy is initially a potentially beneficial response that allows for the normalization of wall pressure and maintenance of cardiac function, if the condition is excessive or prolonged, it can eventually lead to heart failure [9–13]. According to epidemiological studies, cardiac hypertrophy is a critical independent risk factor for arrhythmias, heart failure, and sudden cardiac death, which increases cardiovascular mortality and morbidity [14–20]. Despite enormous efforts to understand the molecular pathophysiology of myocardial hypertrophy and develop effective regimens for its prevention or reversal, no



Copyright: © 2025 by the authors. This is an open access article under the terms and conditions of the Creative Commons Attribution (CC BY) license (<https://creativecommons.org/licenses/by/4.0/>).

Publisher's Note: Scilight stays neutral with regard to jurisdictional claims in published maps and institutional affiliations.

effective treatment is available in clinical settings. Thus, cardiovascular prevention and treatment require investigation of the mechanism of myocardial hypertrophy and development of effective therapeutic drugs.

The calcium-sensing receptor (CaSR), also known as a receptor with seven transmembrane domains, is a G protein-coupled receptor [21]. Wang et al. discovered it in rat heart tissue after cloning it from the bovine parathyroid glands in 1993 [22]. CaSR, the first membrane protein that can sense ions, allows the detection of even the smallest extracellular Ca^{2+} fluctuations in the human body and is crucial in the pathophysiology of cardiovascular disease and Ca^{2+} homeostasis [23,24]. CaSR also influences apoptosis, proliferation, differentiation, migration, and hormone secretion [25–28]. CaSR activation has been associated with the occurrence and progression of vascular calcification, hypertension, and atherosclerosis [29,30]. CaSR overexpression has been linked to the development of cardiac hypertrophy. Several studies have confirmed the ability to inhibit the progression of cardiac hypertrophy in animal models and at the cellular level using the CaSR inhibitor [31,32]. Thus, CaSR may be a significant therapeutic target in myocardial hypertrophy.

Ginseng, a perennial herb belonging to the genus *Panax* (P.), has been used for over 2000 years as a traditional pharmaceutical tonic in China and is widely used as a supplementary medicine in America and Asia [33,34]. Ginsenosides are the main bioactive constituents responsible for most of their pharmacological properties [35]. Several researchers have focused on using individually purified ginsenosides rather than whole ginseng extracts to further investigate the pharmacological effects of ginseng and its underlying rudimentary mechanisms. Ginsenoside Re (Re) (molecular formula: $\text{C}_{48}\text{H}_{82}\text{O}_{18}$, molecular weight: 947.1660), a major ginsenoside extracted from the leaves, roots, and berries of ginseng, is widely used in traditional Chinese medicine (TCM) for cardiovascular diseases [36]. Re has multiple pharmacological activities in vivo and in vitro, including increasing antioxidant enzyme activity, reducing free radicals, and anti-inflammatory and anti-apoptotic [37,38]. Apart from inhibiting ischemic damage to the myocardium by maintaining Ca^{2+} , there is mounting evidence that Re has a beneficial effect on cardiac disease and has also been shown to suppress cardiac hypertrophy and attenuate myocardial damage in experimental heart failure models [39,40]. Re can improve isoproterenol-induced myocardial fibrosis and heart failure by regulating the TGF- β 1/Smad3 pathway and miR-489/myd88/NF- κ B pathway [41,42]. According to preliminary research, Re inhibits myocardial hypertrophy caused by abdominal aortic coarctation by inhibiting CaN and ERK 1 [43]. In this research, we employed an animal model of myocardial hypertrophy using spontaneously hypertensive rats, which more accurately replicates the condition of myocardial hypertrophy in humans resulting from pressure overload. We assessed the therapeutic effects of Re and its influence on the CaSR pathway following 12 weeks of administration via gavage.

2. Materials and Methods

2.1. Animals

Spontaneously hypertensive rats (SHR) and Wistar-Kyoto (WKY) rats were purchased from Vital River Lab Animal Technology at the age of 13 weeks (all males) (certificate number: SCXK 2016–006, Beijing, China). Rats were kept under a daily (12 h/12 h) photoperiod and fed and watered ad libitum for seven days before the experiments. All experiments were approved by the Animal Care and Use Committee of the Zunyi Medical University.

2.2. Chemicals and Reagents

Hengkang Yibai Technology supplied Ginsenoside Re (purity = 96.6%) (Beijing, China). Solarbio Technology Co. Ltd. provided radioimmunoprecipitation assay (RIPA) lysis buffer and nucleoprotein extraction kit (Beijing, China), and Beyotime Biotechnology Co. Ltd. provided BCA Protein Assay Kit (Shanghai, China). Tanon Technology Co., Ltd. provided an enhanced chemiluminescence system (ECL) (Shanghai, China). Santa Cruz Biotechnology (Dallas, TX, USA) provided primary antibodies against atrial natriuretic peptide (ANP, 1:500 dilution, sc-515701), phosphorylated nuclear factor of activated T cells 3 (p-NFAT3, 1: 500 dilution, sc-32630), β -myosin heavy chain (β -MHC, 1: 500 dilution, sc-53090) and phosphorylated zinc finger transcription factor 4 (p-GATA4, 1: 1000 dilution, sc-377543). Abcam (Cambridge, MA, USA) provided the primary antibodies against GATA4 (1: 1000 dilution, ab5245),

calcineurin (CaN, 1: 3000 dilution, ab3673), protein kinase C beta (PKC- β , 1: 1000 dilution, ab23511), rapidly accelerated fibrosarcoma-1 (Raf-1, 1: 1000 dilution, ab33899), and mitogen-activated protein kinase phosphatase-1 (MKP-1, 1: 500 dilution, ab195261). Proteintech (Chicago, IL, USA) provided primary antibodies against extracellular signal-regulated kinase 1/2 (ERK1/2, 1: 2000 dilution, 11257-1-AP), CaSR (1: 1000 dilution, 19125-1-AP), Lamin B1 (1: 3000 dilution, 12987-1-AP), and GAPDH (1: 20000 dilution, 10494-1-AP). Cell Signaling Technology (Beverly, MA, USA) supplied primary antibody against phosphorylated-ERK1/2(p-ERK1/2, 1: 2000 dilution, #4370) and NFAT3 (1: 1000 dilution, #2183).

2.3. Animals and Experimental Protocol

Twenty-four male SHR were randomly assigned to one of the following three groups: model group (SHR), ginsenoside Re 10 mg/kg (Re-10), and ginsenoside Re 20 mg/kg (Re-20). Eight male WKY rats were used as the control group. Distilled water was intragastrically administered to the SHR and WKY groups. The dosage of Re and the course of treatment were determined by our preliminary experiment. Animals were intragastrically administered Re for 12 consecutive weeks.

2.4. Blood Pressure Measurements

We used the tail-cuff technique with the CODA system (Kent Scientific Corp., Torrington, CT, USA) to monitor systolic and diastolic blood pressure in conscious rats. Each group consisted of five rats, and measurements were taken on a weekly basis, following a procedure adapted from the manufacturer's manual. Briefly, rats were placed on a warmed platform for a 15-min stabilization period, after which a series of 15 automated inflation-deflation cycles were initiated, including 5 acclimatization cycles and 10 measurement cycles. The CODA system's software was utilized to calculate and record the systolic and diastolic blood pressure. The mean systolic and diastolic blood pressure was calculated in mmHg.

2.5. Left Ventricular Function Measurements

We randomly assigned three rats from each group for the evaluation of left ventricular function. Prior to the procedure, the rats were anesthetized with an intraperitoneal injection of pentobarbital sodium at a dosage of 30 mg/kg. Subsequently, the chest hair was removed using a depilatory cream to facilitate ultrasonic imaging. Once the hair was cleared, the rats were positioned on an ultrasonic testing platform and the chest area was coated with an appropriate amount of ultrasound gel as a coupling agent. High-resolution echocardiography was performed using the Vevo2100 system (VisualSonics, Toronto, Canada). We measured key cardiac parameters, including the systolic left ventricular internal dimension (LVID; s), diastolic left ventricular internal dimension (LVID; d), ejection fraction (EF), and mean stroke volume (SV).

2.6. Assessment of Indices of Left Ventricle Weight

Following the evaluation of cardiac function, we proceeded with the dissection of the rats to obtain heart tissue samples for further analysis. The chest cavity was opened to fully expose the heart, which was then quickly extracted. We meticulously excised the aorta and any surplus adipose tissue. To eliminate residual blood, the heart was washed in chilled phosphate-buffered saline (PBS) and patted dry with absorbent filter paper. The left and right ventricles were then carefully isolated, their weights were precisely measured, and the data was documented.

To quantify the degree of left ventricular hypertrophy, we calculated two indices: the Left Ventricular Hypertrophy Index (LVHI) by dividing the weight of the left ventricle by the rat's body weight, and the ratio of Left Ventricular Weight to Right Ventricular Weight (LVW/RVW) by dividing the weight of the left ventricle by that of the right ventricle.

2.7. Histological Analysis

A portion of rat left ventricular tissue was carefully clipped and immediately fixed in 4% paraformaldehyde for 48 h, dehydrated in a gradient series of ethanol, and then paraffin-embedded. HE staining was performed on 3.5-micron sections according to the kit instructions. Briefly, the sections were

dried in an oven at 70 °C to remove moisture and residual paraffin, dewaxed in xylene, rehydrated through a graded series of ethanol (100%, 95%, 80%, and 70%), and rinsed in running water for 10 min. They were then stained with hematoxylin staining solution for 5 min, washed with tap water to remove excess staining solution, differentiated in hydrochloric acid and alcohol for 30 s, and washed in tap water until the nuclei were clear. Subsequently, the sections were stained with eosin staining solution for 2 min, washed again with tap water to remove excess staining solution, dehydrated through a series of ethanol concentrations, cleared in xylene, and finally mounted with a coverslip using a synthetic resin. The samples were then air-dried. An image analysis system (BX 43; Olympus, Tokyo, Japan) was used to detect pathological changes in the myocardium. The cross-sectional area of each left ventricular section was calculated using Image Pro-Plus and a minimum of 60 cardiomyocytes.

2.8. Extraction of Cytoplasmic and Nuclear Proteins

The protocol supplied with nucleoprotein extraction kit was used to extract cytoplasmic and nuclear protein fractions. First, frozen left ventricular tissues were weighed and homogenized in ice-cold PBS. The homogenates were then centrifuged (500× g, 3 min, 4 °C) to collect the sediment, which was mixed with the plasma protein extraction reagent. The mixture was spun in a high-speed vortex for approximately 30 s before being placed on ice for 10 min and centrifuged (16,000× g for 10 min at 4 °C). Finally, supernatants containing cytoplasmic protein fractions were obtained. The sediment was treated with a nucleoprotein extraction reagent. After 10 min on ice, the mixture was centrifuged (16,000× g for 10 min at 4 °C). Supernatants containing nuclear protein fractions were collected.

2.9. Western Blotting

Five rats were randomly chosen for the western blot analysis. Radioimmunoprecipitation assay (RIPA) buffer was used to extract proteins from tissue homogenates. The homogenates were centrifuged at 12,000 rpm at 4 °C, and the supernatants were collected and stored at –80 °C. Protein concentrations in the samples were determined using a BCA assay kit. The next step was to evaluate aliquots of supernatants containing the same amount of protein (30 µg). We assayed the expression of ANP, β-MHC, CaSR, CaN, GATA4, p-GATA4, NFAT3, p-NFAT3, Raf-1, PKC-β, ERK1/2, p-ERK1/2, MKP-1, Lamin B1, and GAPDH. ANP, β-MHC, CaSR, CaN, p-NFAT3, PKC-β, Raf-1, and MKP-1 expression levels were normalized to GAPDH expression. The expression of NFAT3 was normalized to the expression of Lamin B1. The p-GATA4 and p-ERK1/2 levels were normalized to GATA4 and ERK1/2 basal levels. After washing, the blots were incubated at room temperature for 2 h with species-specific horseradish peroxidase (HRP) -labeled secondary antibodies. Protein visualization was accomplished using an ECL western blotting system. Each immunoblot was quantified using a gel imaging and analysis system and Quantity One 1-D Analysis Software (v4.52, Bio-Rad).

2.10. Molecular Docking

Molecular docking calculations were performed using AutoDock 4.2, and the affinity between Re and CaSR was observed using AutoDockTools software. Three-dimensional (3D) protein structures of CaSR (PDB ID:7SIL) were retrieved from the Protein Data Bank (<https://doi.org/10.2210/pdb7sil/pdb>). (Accessed on 15th. Mar. 2024)). Molecular docking of the Re and CaSR binding sites was analyzed using AutoDock software.

3. Statistical Analyses

The data are expressed as the mean ±SEM, and the analyses were carried out using SPSS 18.0. One-way analysis of one-way ANOVA was used to statistically analyze the data. In the case of homogeneity of variance, the least significant difference (LSD) test was used, whereas in the case of heterogeneity of variance, Dunnett's T3 test was used. When $p < 0.05$, Differences were considered statistically significant.

4. Result

4.1. Re Inhibited the Increase of Blood Pressure in SHR

With increasing age, the blood pressure of SHR also increases continuously. To observe the establishment of the SHR model and the effect of Re on the blood pressure of rats, we used the CODA Non-Invasive BP System to monitor the tail arterial pressure. As shown in Figure 1, the blood pressure of WKY rats was relatively stable during the monitoring period of 14–26 weeks. Both systolic and diastolic pressures increased with age in the SHR group, but a 12-week intervention with Re effectively reduced the blood pressure of the SHR, especially in the Re 20 mg/kg group ($p < 0.05$).

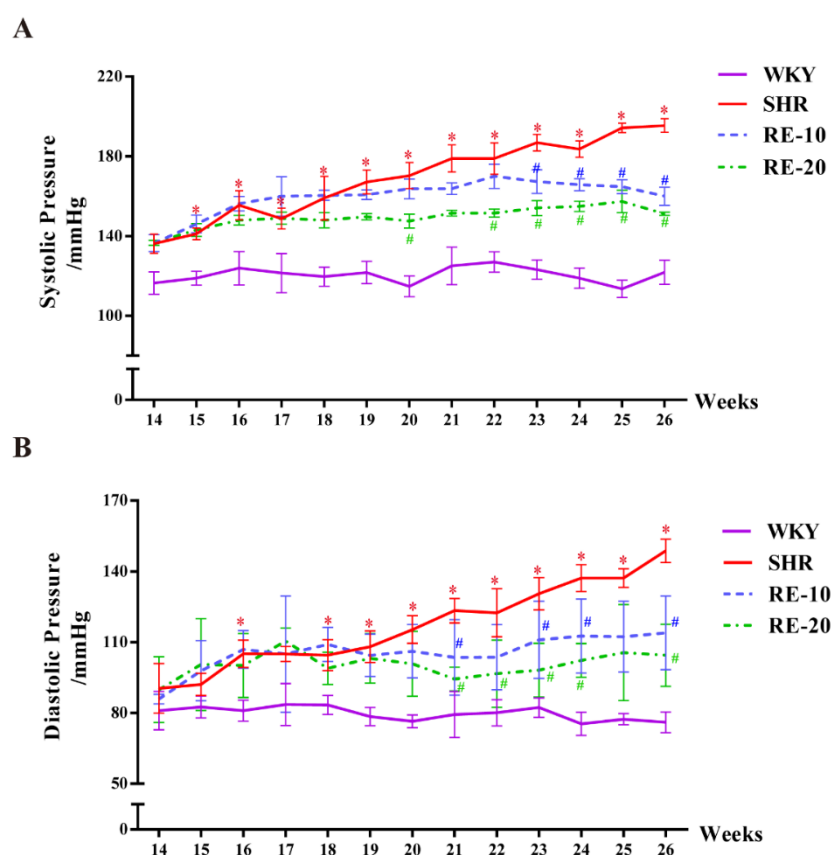


Figure 1. Systolic and diastolic blood pressures were measured using the CODA Non-Invasive Blood Pressure System in both WKY and SHR. ($n = 5$). (A) Changes in systolic pressure over the 12 weeks period among four experimental groups. (B) Changes in diastolic pressure over the 12 weeks period among four experimental groups. Data are presented as mean \pm SEM. * significantly different from WKY rats at $p < 0.05$; # significantly different from SHR at $p < 0.05$.

4.2. Re Attenuates Left Ventricular Structure and Function in SHR

To observe the formation of cardiac hypertrophy in rats more intuitively, changes in cardiac structure in each group were observed using a high-resolution ultrasonic imaging system. Compared to WKY rats, the SHR group had a significantly lower LVID; d, LVID; s, EF, and SV ($p < 0.05$). (Table 1, Figure 2). Under these experimental conditions, the decrease in ventricular diameter and stroke volume reflects the impairment of cardiac function and occurrence of myocardial hypertrophy. We found significant increases in EF, SV, LVID; d, and LVID; s after 12 weeks of Re administration ($p < 0.05$).

Table 1. Echocardiography-related data in SHR rats after 12 weeks of Re treatment.

Group	LVID; d (mm)	LVID; s (mm)	EF (%)	SV (μL)
WKY	6.52 ± 0.13	3.43 ± 0.24	95.11 ± 3.58	120.62 ± 7.94
SHR	4.46 ± 0.10 *	1.98 ± 0.09 *	62.57 ± 2.33 *	75.62 ± 0.61 *
RE-10	4.54 ± 0.38	2.66 ± 0.32 #	80.73 ± 3.99 #	76.68 ± 7.58
RE-20	5.65 ± 0.19 #	3.36 ± 0.50 #	93.37 ± 2.75 #	111.41 ± 14.51 #

Fourteen-week-old rats were administered ginsenoside Re via gavage for a period of 12 weeks. Echocardiographic analysis was employed to evaluate the development of myocardial hypertrophy in these rats. (LVID; d: Diastole of the left ventricular internal dimension thickness. LVID; s: Systole of the left ventricular internal dimension thickness. EF: Ejection fraction. SV: Average cardiac stroke volume. Data are presented as mean ± SEM. * significantly different from WKY rats at $p < 0.05$; # significantly different from SHR at $p < 0.05$.

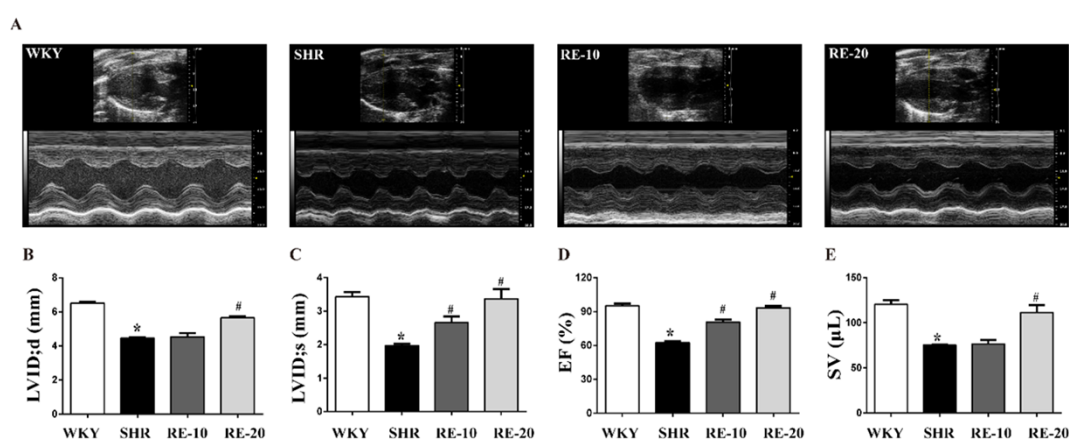


Figure 2. Re attenuates left ventricular structure and function in SHR. Left ventricular hypertrophy was determined by echocardiography after 12 weeks of drug administration. (n = 3). (A) Representative echocardiograms are shown. (B) Diastole of the left ventricular internal dimension (LVID; d) thickness. (C) Systole of the left ventricular internal dimension (LVID; s) thickness. (D) Ejection fraction (EF). (E) Average cardiac stroke volume (SV). Data are presented as mean ± SEM. * significantly different from WKY rats at $p < 0.05$; # significantly different from SHR at $p < 0.05$.

4.3. Re Decreases the Left Ventricle Hypertrophic Indexes in SHR

Figure 3 shows that in contrast to the WKY group, the SHR group showed significant increases in hypertrophic indicators (including LVHI and LVW/RVW) at 26 weeks of age ($p < 0.05$). The increase in left ventricular weight in SHR indicates that cardiac protein synthesis increases, cell volume increases, and myocardial hypertrophy occurs. These indices decreased after Re treatment ($p < 0.05$).

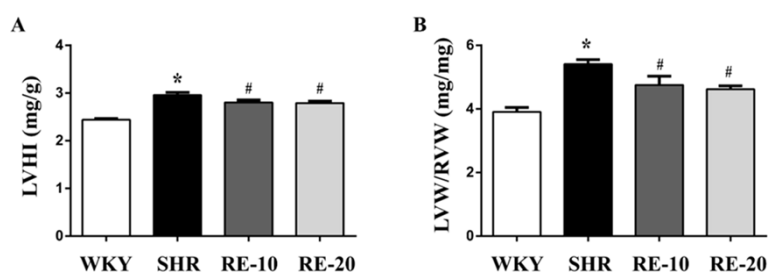


Figure 3. Re decreased hypertrophic parameters of SHR. (n = 8). (A) The ratio of left ventricle weight/ body weight (LVHI). (B) Left ventricle weight/ right ventricle weight (LVW/RVW). Data are presented as mean ± SEM. * significantly different from WKY rats at $p < 0.05$; # significantly different from SHR at $p < 0.05$.

4.4. Re Alleviates Cardiac Hypertrophy in SHR

To observe the changes in the left ventricular pathomorphology in rats, HE staining was used to observe

the cross-sectional area of the cardiomyocytes. As shown in Figure 4, SHR had a significantly larger mean cross-sectional area of cardiomyocytes than WKY rats ($p < 0.05$). In contrast, the Re treatment groups had significantly smaller cross-sectional areas than the SHR group ($p < 0.05$).

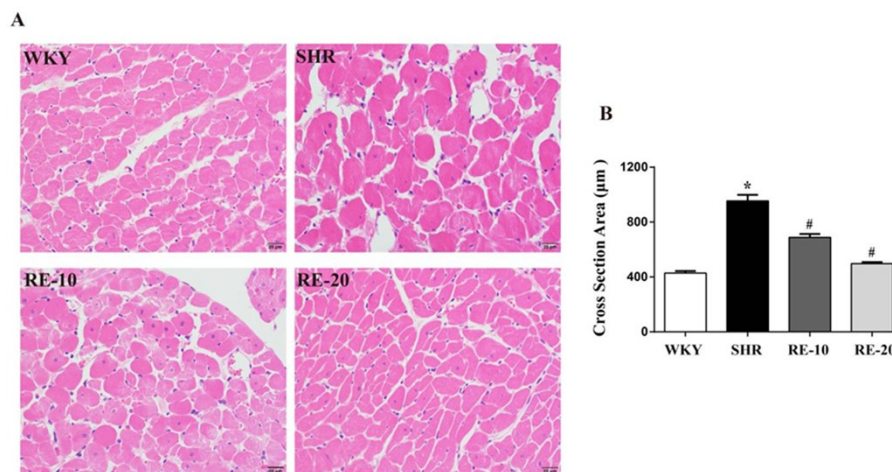


Figure 4. Re reverses cardiac hypertrophy in SHR. (n = 5). (A) Representative images of H&E staining of cardiac tissue from the WKY, SHR, Re-10, Re-20 groups. Scale bar = 20 µm. (B) Quantified cross-sectional areas of cardiomyocytes from the WKY, SHR, Re-10, Re-20 groups. Data are presented as mean ± SEM. * significantly different from WKY rats at $p < 0.05$; # significantly different from SHR at $p < 0.05$.

4.5. Re reduces the Expressions of ANP and β-MHC

ANP and MHC are two markers of myocardial hypertrophy, and their expression was detected using western blotting. As shown in Figure 5, SHR showed significantly higher levels of ANP and β-MHC protein expression. Administration of Re for 12 weeks significantly reduced the expression of these proteins, with a more prominent effect observed in the group treated with 20 mg/kg Re ($p < 0.05$).

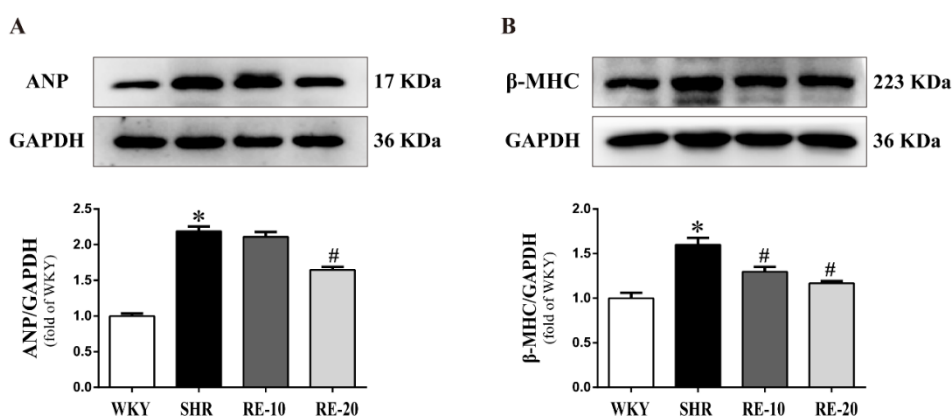


Figure 5. Re downregulates ANP and β-MHC in the myocardial tissue of SHR. (n = 5). (A) quantitative analysis of ANP protein levels. (B) quantitative analysis of β-MHC protein levels. Data are presented as mean ± SEM. * significantly different from WKY rats at $p < 0.05$; # significantly different from SHR at $p < 0.05$.

4.6. Re Suppresses the CaSR Signaling Pathway in SHR

Previous studies have demonstrated that the CaSR is involved in the progression of myocardial hypertrophy. To elucidate the potential mechanisms that may be involved in mediating the protective effects of Re, we performed western blotting to detect the expression of the CaSR-mediated signaling pathway. As shown in Figure 6, the SHR had higher levels of CaSR, CaN, NFAT3, and p-GATA4 proteins in the myocardium. ($p < 0.05$). Meanwhile, cytoplasmic p-NFAT3 protein levels in SHR decreased dramatically

($p < 0.05$). Re administration significantly reduced CaSR, CaN, NFAT3, and p-GATA4 expression in the left ventricular myocardial tissues and increased cytoplasmic p-NFAT3 protein expression in SHR aged 26 weeks, with a more pronounced effect observed in the group treated with 20 mg/kg Re ($p < 0.05$).

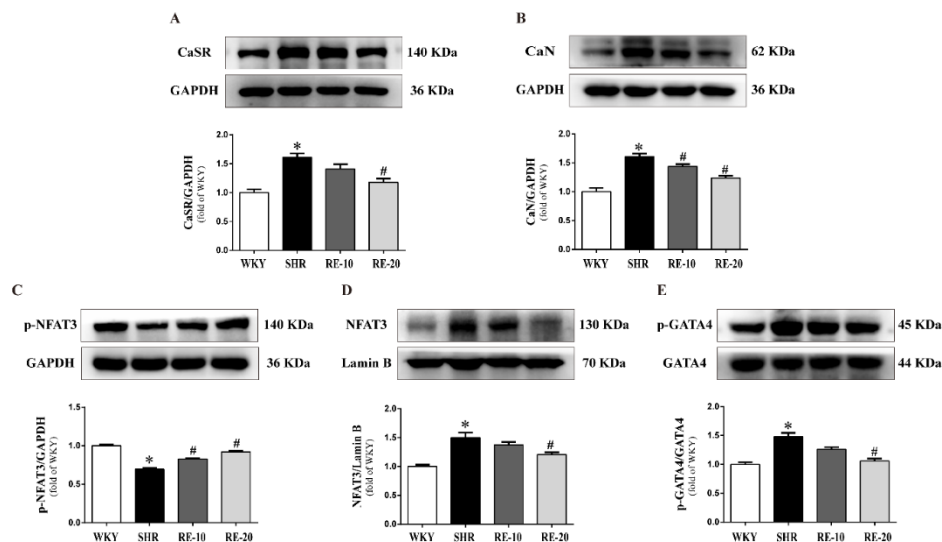


Figure 6. Re suppresses the CaSR signaling pathway in SHR. (n = 5). (A) Quantitative analysis of CaSR protein levels. (B) Quantitative analysis of CaN protein levels. (C) Quantitative analysis of p-NFAT3 protein levels. (D) Quantitative analysis of NFAT3 protein levels. (E) Quantitative analysis of p-GATA4 protein levels. Data are presented as mean \pm SEM. * significantly different from WKY rats at $p < 0.05$; # significantly different from SHR at $p < 0.05$.

4.7. Re Suppresses the PKC-MAPK Signaling Pathway in SHR

As shown in Figure 7, the myocardial expression of PKC- β , Raf-1, and p-ERK1/2 proteins was significantly elevated in SHR, whereas MKP-1 levels decreased dramatically ($p < 0.05$). Re significantly decreased the expression of PKC- β , Raf-1, and p-ERK1/2, while significantly increasing MKP-1 levels in left ventricular myocardial tissues ($p < 0.05$).

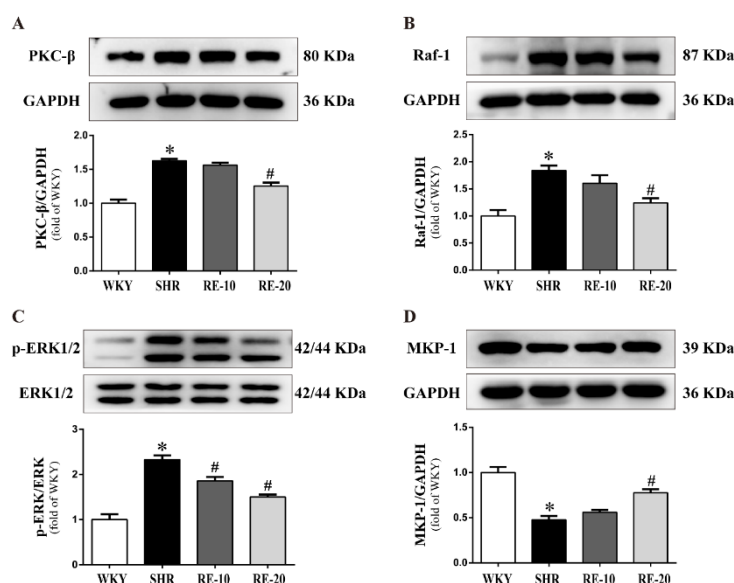


Figure 7. Re suppresses the PKC-MAPK signaling pathway in SHR. (n = 5). (A) Quantitative analysis of PKC- β protein levels. (B) Quantitative analysis of Raf-1 protein levels. (C) Quantitative analysis of p-ERK1/2 protein levels. (D) Quantitative analysis of MKP-1 protein levels. Data are presented as mean \pm SEM. * significantly different from WKY rats at $p < 0.05$; # significantly different from SHR at $p < 0.05$.

4.8. Re Bound to and Inhibited CaSR

Molecular docking analysis was performed to confirm whether Re bound to the CaSR protein. Our findings demonstrated that the binding energy of Re and CaSR was -7.7 kcal/mol, which verified that Re directly bound to CaSR. We further explored the possible binding modes and interactions within the amino acid pocket of CaSR, including SER 303, GLU 405, and ASP 410 (Figure 8). These results indicate that Re may directly affect CaSR and attenuate cardiac hypertrophy.

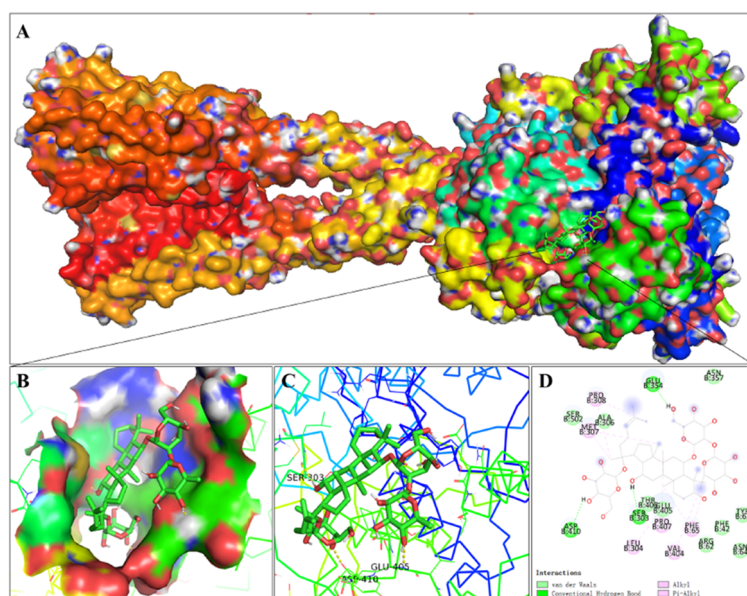


Figure 8. Re bound and inhibited CaSR. (A) A visual of the binding sites between Re and CaSR. (B, C) Close-up view of the molecular binding pocket. (D) Amino acid residues.

5. Discussion

Myocardial hypertrophy is not only a risk factor for human health but also a predictor of increased cardiovascular mortality [44,45]. It is a risk factor for cardiac arrhythmia and increases the risk of a heart attack. Therefore, it is critical to study the pathogenesis of myocardial hypertrophy [46]. However, hypertension-induced cardiac pressure overload is a major pathogenic factor for myocardial hypertrophy in the hypertensive population. SHR are a well-known genetic murine model of hypertension that closely resemble human hypertension. Hypertensive rats frequently exhibit cardiac hypertrophy [47].

SHR show a progressive increase in blood pressure with age [48,49]. The current study showed a significant increase in the rats' left ventricle hypertrophic indices in rats. In contrast to WKY rats, SHR showed a significant decrease in EF, SV, LVID; d, and LVID; s and a significantly increased cardiomyocyte cross-sectional area. These findings indicate impaired left ventricle function and morphology in the SHR. Significant increases in ANP and β -MHC, two biomarkers of myocardial hypertrophy, were also observed in the SHR myocardial tissues. These findings indicate that persistent hypertension causes myocardial hypertrophy, consistent with our previous study [50]. Increasing evidence suggests that ginseng extract improves the vascular biology of animals with normal and high blood pressures [51–53]. In the current study, we discovered that Re treatment for 12 weeks significantly increased LVID; d, LVID; s, EF, and SV; decreased hypertrophic indexes, such as LVHI and LVW/RVW; decreased the average cross-sectional area of myocardial cells; and decreased the expression of ANP and β -MHC proteins. These findings indicate that Re protects against myocardial hypertrophy in SHR.

Hypertrophy have been linked to the calcium homeostasis and CaSR in the vasculature. For example, CaSR activation leads to the activation of pathways that are calcium ion dependent, such as Ca^{2+} /calmodulin-dependent protein kinase II (CaMKII) and calcineurin pathways [54]. Other studies demonstrated that treatment of an isoprenaline (ISO)-induced cardiac hypertrophy model using the CaSR inhibitor Calhex231

revealed amelioration of myocardial hypertrophy in Calhex231-treated rats, with similar results obtained at the cellular level [32]. Based on this, we conclude that the calcium-sensing receptor (CaSR) plays a significant role in cardiac hypertrophy, and modulation of CaSR-mediated signaling pathways may have an anti-hypertrophic effect on the heart.

When myocardial hypertrophy occurs, extracellular Ca^{2+} activates CaSR, which belongs to the G protein-coupled receptor family. This, in turn, stimulates phospholipase C (PLC)- β to mediate phosphatidylinositol 4,5-bisphosphate hydrolysis, resulting in the secondary messengers inositol 1, 4, 5-triphosphate (IP3) and diacylglycerol (DAG) [55 – 57]. IP3 causes the release of $[\text{Ca}^{2+}]_i$ from intracellular stores, such as the endoplasmic reticulum, which further activates CaN. The NFAT3 protein, which is found in the cytoplasm of resting cells, is phosphorylated. When stimulated, CaN dephosphorylates this protein, causing it to translocate to the nucleus. The activation of its transcriptional activity establishes a direct link between intracellular Ca^{2+} signaling and gene expression. NFAT3 interacts with cardiac p-GATA4 and cardiac transcription is synergistically activated. Finally, myocardial hypertrophy markers ANP and β -MHC were upregulated. In the present study, Re reduced the levels of CaSR, CaN, NFAT3, and p-GATA4 while increasing the levels of p-NFAT3 in the myocardium of SHR.

PKC was activated by DAG alone or in combination with $[\text{Ca}^{2+}]_i$. The mitogen- activated protein kinase (MAPK) axis is activated by the G protein-coupled receptor. PKC- β stimulation promotes the initiation of Raf-1 and MAPK pathways. ERK1/2, a member of the MAPK family, is associated with myocardial hypertrophy. After phosphorylation, it binds to GATA4, which can be inhibited by MKP-1 [58]. In this study, PKC- β , Raf-1, and p-ERK1/2 protein levels were elevated in the SHR group, whereas MKP-1 protein levels were decreased. Treatment with Re for 12 weeks reduced this effect.

This finding underscores the potential of ginsenoside Re to be used either as a standalone treatment or alongside other medications, laying the groundwork for developing ginsenoside-based therapies for cardiac hypertrophy management. However, the study has some limitations. Firstly, it would have been improved by including a larger number of animals and employing various experimental methods across a wider sample size to strengthen the results. Second, the anti-myocardial hypertrophic effect of Re needs to be further validated by in vitro studies, as well as the use of CaSR-specific inhibitors to compare the efficacy of Re. Future research should utilize a broader range of experimental models and techniques, including CaSR knockout models both in vivo and in vitro. Additionally, a thorough investigation into the mechanisms behind the anti-hypertrophic effects of ginsenoside Re should be carried out using techniques such as genetic sequencing, immunoprecipitation, and immunofluorescence.

In summary, our research indicates that ginsenoside Re possesses the capacity to mitigate cardiac hypertrophy through the modulation of the PKC-MAPK signaling pathway and CaSR-mediated signaling pathways (Figure 9).

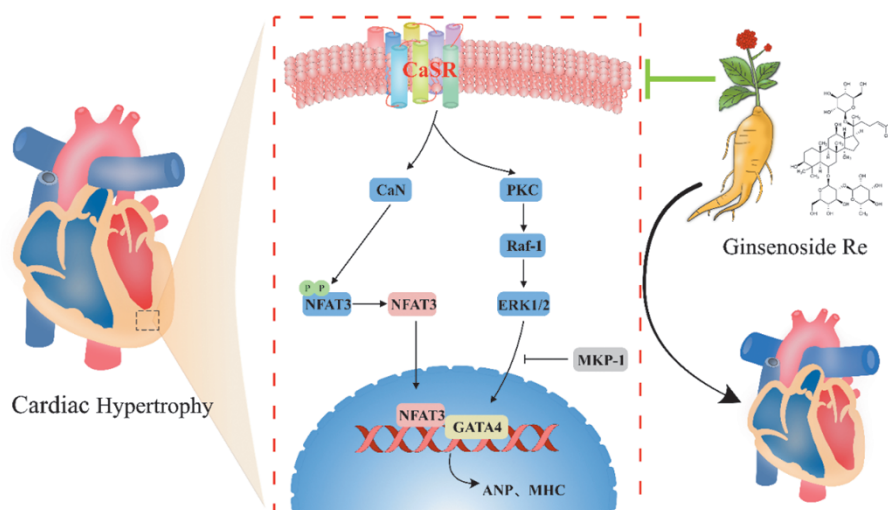


Figure 9. Schematic diagram of the mechanism underlying inhibition of cardiac hypertrophy by Re in SHR.

Author Contributions: P.C. and M.L. performed the experiments. H.X. and Z.L. assisted with this experiment. T.L., H.L. and X.C. performed statistical analysis. P.C. wrote the manuscript, with the help of S.X. and Z.L. J.D. designed the experiments and revised the manuscript accordingly. All authors contribute to manuscript revision and have read and approved the submitted version.

Funding: This study was supported by the National Natural Science Foundation of China (Grant Nos. 81860732 and 82060682), the State Key Laboratory of Cardiovascular Disease (Grant No. 2017kf-03), and the Zunyi Science and Technology Bureau of Guizhou Province [Zunshi Kehe HZ (2022) No. 191].

Institutional Review Board Statement: This study was conducted in accordance with the Guide for the Care and Use of Laboratory Animals as promulgated by the National Institutes of Health, and the protocols were approved by the Animal Care and Use Committee of Zunyi Medical University (No.[2020] 2-026).

Informed Consent Statement: Not applicable.

Data Availability Statement: The data supporting the findings of this study are available from the corresponding author upon reasonable request.

Conflicts of Interest: The authors declare no conflict of interest.

References

1. Zhang, Y.; Da, Q.; Cao, S.; et al. HINT1 (Histidine Triad Nucleotide-Binding Protein 1) Attenuates Cardiac Hypertrophy Via Suppressing HOXA5 (Homeobox A5) Expression. *Circulation* **2021**, *144*, 638–654.
2. Oldfield, C.J.; Duhamel, T.A.; Dhalla, N.S. Mechanisms for the transition from physiological to pathological cardiac hypertrophy. *Can. J. Physiol. Pharmacol.* **2020**, *98*, 74–84.
3. Yoshida, K.; Holmes, J.W. Computational models of cardiac hypertrophy. *Prog. Biophys. Mol. Biol.* **2021**, *159*, 75–85.
4. Jin, L.; Piao, Z.H.; Liu, C.P.; et al. Gallic acid attenuates calcium calmodulin-dependent kinase II-induced apoptosis in spontaneously hypertensive rats. *J. Cell. Mol. Med.* **2018**, *22*, 1517–1526.
5. Deng, K.Q.; Zhao, G.N.; Wang, Z.; et al. Targeting Transmembrane BAX Inhibitor Motif Containing 1 Alleviates Pathological Cardiac Hypertrophy. *Circulation* **2018**, *137*, 1486–1504.
6. Meng, G.; Liu, J.; Liu, S.; et al. Hydrogen sulfide pretreatment improves mitochondrial function in myocardial hypertrophy via a SIRT3-dependent manner. *Br. J. Pharmacol.* **2018**, *175*, 1126–1145.
7. Bazgir, F.; Nau, J.; Nakhaei-Rad, S.; et al. The Microenvironment of the Pathogenesis of Cardiac Hypertrophy. *Cells* **2023**, *12*, 1780.
8. Zhu, M.; Hu, J.; Pan, Y.; et al. Magnoflorine attenuates Ang II-induced cardiac remodeling via promoting AMPK-regulated autophagy. *Cardiovasc. Diagn. Ther.* **2024**, *14*, 576–588.
9. Martin, T.G.; Juarros, M.A.; Leinwand, L.A. Regression of cardiac hypertrophy in health and disease: Mechanisms and therapeutic potential. *Nat. Rev. Cardiol.* **2023**, *20*, 347–363.
10. Tang, X.; Pan, L.; Zhao, S.; et al. SNO-MLP (S-Nitrosylation of Muscle LIM Protein) Facilitates Myocardial Hypertrophy Through TLR3 (Toll-Like Receptor 3)-Mediated RIP3 (Receptor-Interacting Protein Kinase 3) and NLRP3 (NOD-Like Receptor Pyrin Domain Containing 3) Inflammasome Activation. *Circulation* **2020**, *141*, 984–1000.
11. Gallo, S.; Vitacolonna, A.; Bonzano, A.; et al. ERK: A Key Player in the Pathophysiology of Cardiac Hypertrophy. *Int. J. Mol. Sci.* **2019**, *20*, 2164.
12. Jin, L.; Sun, S.; Ryu, Y.; et al. Gallic acid improves cardiac dysfunction and fibrosis in pressure overload-induced heart failure. *Sci. Rep.* **2018**, *8*, 9302.
13. Ritterhoff, J.; Tian, R. Metabolic mechanisms in physiological and pathological cardiac hypertrophy: New paradigms and challenges. *Nat. Rev. Cardiol.* **2023**, *20*, 812–829.
14. Luo, Y.; Jiang, N.; May, H.I.; et al. Cooperative Binding of ETS2 and NFAT Links Erk1/2 and Calcineurin Signaling in the Pathogenesis of Cardiac Hypertrophy. *Circulation* **2021**, *144*, 34–51.
15. Patel, S.K.; Ramchand, J.; Crocitti, V.; et al. Kruppel-Like Factor 15 Is Critical for the Development of Left Ventricular Hypertrophy. *Int. J. Mol. Sci.* **2018**, *19*, 1303.
16. Shimizu, I.; Minamino, T. Physiological and pathological cardiac hypertrophy. *J. Mol. Cell. Cardiol.* **2016**, *97*, 245–262.
17. Zhang, J.; Sun, J.; Gu, X.; et al. Transcriptome sequencing analysis reveals the molecular regulatory mechanism of myocardial hypertrophy induced by angiotensin II. *Biochem. Pharmacol.* **2024**, *229*, 116532.
18. Stanko, P.; Repova, K.; Baka, T.; et al. Sacubitril/Valsartan Alleviates Cardiac Remodeling and Dysfunction in L-NAME-Induced Hypertension and Hypertensive Heart Disease. *Biomedicines* **2024**, *12*, 733.
19. Eghan, P.; Folsom, A.A.; Donkor, A.; et al. Relationship between hypertensive disorders of pregnancy (HDP) and cardiac remodeling during pregnancy: Systematic review and meta-analysis. *Eur. J. Obstet. Gynecol. Reprod. Biol.* **2024**, *298*, 108–115.
20. Zhang, B.B.; Zhao, Y.L.; Lu, Y.Y.; et al. TMEM100 acts as a TAK1 receptor that prevents pathological cardiac hypertrophy progression. *Cell Commun. Signal.* **2024**, *22*, 438.
21. Brown, E.M.; Gamba, G.; Riccardi, D.; et al. Cloning and characterization of an extracellular Ca²⁺-sensing receptor from bovine parathyroid. *Nature* **1993**, *366*, 575–580.

22. Wang, R.; Xu, C.; Zhao, W.; et al. Calcium and polyamine regulated calcium-sensing receptors in cardiac tissues. *Eur. J. Biochem.* **2003**, *270*, 2680–2688.
23. Schreckenber, R.; Schlüter, K.D. Calcium sensing receptor expression and signalling in cardiovascular physiology and disease. *Vasc. Pharmacol.* **2018**, *107*, 35–42.
24. Pollak, M.R.; Brown, E.M.; Chou, Y.H.; et al. Mutations in the human Ca⁽⁺⁺⁾-sensing receptor gene cause familial hypocalciuric hypercalcemia and neonatal severe hyperparathyroidism. *Cell* **1993**, *75*, 1297–1303.
25. Zhou, M.Y.; Cheng, L.; Chen, L.; et al. Calcium-sensing receptor in the development and treatment of pulmonary hypertension. *Mol. Biol. Rep.* **2021**, *48*, 975–981.
26. Tharmalingam, S.; Hampson, D. R. The Calcium-Sensing Receptor and Integrins in Cellular Differentiation and Migration. *Front. Physiol.* **2016**, *7*, 190.
27. Owen, J.L.; Cheng, S.X.; Ge, Y.; et al. The role of the calcium-sensing receptor in gastrointestinal inflammation. *Semin. Cell Dev. Biol.* **2016**, *49*, 44–51.
28. Zeng, J.; Cheng, Y.; Xie, W.; et al. Calcium-sensing receptor and NF-κB pathways in TN breast cancer contribute to cancer-induced cardiomyocyte damage via activating neutrophil extracellular traps formation. *Cell. Mol. Life Sci. CMLS* **2024**, *81*, 19.
29. Hendy, G.N.; Canaff, L. Calcium-sensing receptor, proinflammatory cytokines and calcium homeostasis. *Semin. Cell Dev. Biol.* **2016**, *49*, 37–43.
30. Diaz-Soto, G.; Roher, A.; Garcia-Rodríguez, C.; et al. The Calcium-Sensing Receptor in Health and Disease. *Int. Rev. Cell Mol. Biol.* **2016**, *327*, 321–369.
31. Sundararaman, S.S.; van der Vorst, E.P.C. Calcium-Sensing Receptor (CaSR), Its Impact on Inflammation and the Consequences on Cardiovascular Health. *Int. J. Mol. Sci.* **2021**, *22*, 2478.
32. Liu, L.; Wang, C.; Lin, Y.; et al. Suppression of calcium-sensing receptor ameliorates cardiac hypertrophy through inhibition of autophagy. *Mol. Med. Rep.* **2016**, *14*, 111–120.
33. Jiang, J.; Sun, X.; Akther, M.; et al. Ginsenoside metabolite 20(S)-protopanaxatriol from Panax ginseng attenuates inflammation-mediated NLRP3 inflammasome activation. *J. Ethnopharmacol.* **2020**, *251*, 112564.
34. Xu, X.; Jin, L.; Jiang, T.; et al. Ginsenoside Rh2 attenuates microglial activation against toxoplasmic encephalitis via TLR4/NF-κB signaling pathway. *J. Ginseng Res.* **2020**, *44*, 704–716.
35. Sarhene, M.; Ni, J. Y.; Duncan, E. S.; et al. Ginsenosides for cardiovascular diseases; update on pre-clinical and clinical evidence, pharmacological effects and the mechanisms of action. *Pharmacol. Res.* **2021**, *166*, 105481.
36. Gao, X.Y.; Liu, G.C.; Zhang, J.X.; et al. Pharmacological Properties of Ginsenoside Re. *Front. Pharmacol.* **2022**, *13*, 754191.
37. Lee, G.H.; Lee, W.J.; Hur, J.; et al. Ginsenoside Re Mitigates 6-Hydroxydopamine-Induced Oxidative Stress through Upregulation of GPX4. *Molecules* **2020**, *25*, 188.
38. Liu, M.; Bai, X.; Yu, S.; et al. Ginsenoside Re Inhibits ROS/ASK-1 Dependent Mitochondrial Apoptosis Pathway and Activation of Nrf2-Antioxidant Response in Beta-Amyloid-Challenged SH-SY5Y Cells. *Molecules* **2019**, *24*, 2687.
39. Wang, Q.W.; Yu, X.F.; Xu, H.L.; et al. Ginsenoside Re Attenuates Isoproterenol-Induced Myocardial Injury in Rats. *Evid. -Based Complement. Altern. Med.* **2018**, *2018*, 8637134.
40. Yu, Y.; Sun, J.; Liu, J.; et al. Ginsenoside Re Preserves Cardiac Function and Ameliorates Left Ventricular Remodeling in a Rat Model of Myocardial Infarction. *J. Cardiovasc. Pharmacol.* **2020**, *75*, 91–97.
41. Wang, Q.W.; Yu, X.F.; Xu, H.L.; et al. Ginsenoside Re Improves Isoproterenol-Induced Myocardial Fibrosis and Heart Failure in Rats. *Evid. -Based Complement. Altern. Med.* **2019**, *2019*, 3714508.
42. Sun, J.; Wang, R.; Chao, T.; et al. Ginsenoside Re inhibits myocardial fibrosis by regulating miR-489/myd88/NF-κB pathway. *J. Ginseng Res.* **2023**, *47*, 218–227.
43. He, Y. Effect of Ginsenoside Re on Left Ventricular Hypertrophy Induced by Aortic Coarctation in Rats. Master's Thesis, Zunyi Medical University, Zunyi, China, 2009.
44. Smith, K.M.; Squiers, J. Hypertrophic cardiomyopathy: An overview. *Crit. Care Nurs. Clin. N. Am.* **2013**, *25*, 263–272.
45. Oka, T.; Akazawa, H.; Naito, A.T.; et al. Angiogenesis and cardiac hypertrophy: Maintenance of cardiac function and causative roles in heart failure. *Circ. Res.* **2014**, *114*, 565–571.
46. Ren, B.; Feng, J.; Yang, N.; et al. Ginsenoside Rg3 attenuates angiotensin II-induced myocardial hypertrophy through repressing NLRP3 inflammasome and oxidative stress via modulating SIRT1/NF-κB pathway. *Int. Immunopharmacol.* **2021**, *98*, 107841.
47. Damatto, R.L.; Lima, A.R.; Martinez, P.F.; et al. Myocardial myostatin in spontaneously hypertensive rats with heart failure. *Int. J. Cardiol.* **2016**, *215*, 384–387.
48. Elmarakby, A. A.; Sullivan, J. C. Sex differences in hypertension: Lessons from spontaneously hypertensive rats (SHR). *Clin. Sci.* **2021**, *135*, 1791–1804.
49. Fu, S.; Li, Y.L.; Wu, Y.T.; et al. Icariside II attenuates myocardial fibrosis by inhibiting nuclear factor-κB and the TGF-β1/Smad2 signalling pathway in spontaneously hypertensive rats. *Biomed. Pharmacoth.* **2018**, *100*, 64–71.
50. Chen, P.; Wen, Z.; Shi, W.; et al. Effects of Sodium Ferulate on Cardiac Hypertrophy Are via the CaSR-Mediated Signaling Pathway. *Front. Pharmacol.* **2021**, *12*, 674570.
51. Lee, H.J.; Kim, B.M.; Lee, S.H.; et al. Ginseng-Induced Changes to Blood Vessel Dilation and the Metabolome of Rats. *Nutrients* **2020**, *12*, 2238.
52. Vuksan, V.; Xu, Z.Z.; Jovanovski, E.; et al. Efficacy and safety of American ginseng (*Panax quinquefolius* L.) extract on glycemic control and cardiovascular risk factors in individuals with type 2 diabetes: A double-blind, randomized,

- cross-over clinical trial. *Eur. J. Nutr.* **2019**, *58*, 1237–1245.
53. Zhu, G.X.; Zuo, J.L.; Xu, L.; et al. Ginsenosides in vascular remodeling: Cellular and molecular mechanisms of their therapeutic action. *Pharmacol. Res.* **2021**, *169*, 105647.
54. Lu, M.; Leng, B.; He, X.; et al. Calcium Sensing Receptor-Related Pathway Contributes to Cardiac Injury and the Mechanism of Astragaloside IV on Cardioprotection. *Front. Pharmacol.* **2018**, *9*, 1163.
55. Leach, K.; Hannan, F. M.; Josephs, T. M.; et al. International Union of Basic and Clinical Pharmacology. CVIII. Calcium-Sensing Receptor Nomenclature, Pharmacology, and Function. *Pharmacol. Rev.* **2020**, *72*, 558–604.
56. Hong, S.; Zhang, X.; Zhang, X.; et al. Role of the calcium sensing receptor in cardiomyocyte apoptosis via mitochondrial dynamics in compensatory hypertrophied myocardium of spontaneously hypertensive rat. *Biochem. Biophys. Res. Commun.* **2017**, *487*, 728–733.
57. Tian, L.; Andrews, C.; Yan, Q.; et al. Molecular regulation of calcium-sensing receptor (CaSR)-mediated signaling. *Chronic Dis. Transl. Med.* **2024**, *10*, 167–194.
58. Hu, B.; Song, J.T.; Ji, X.F.; et al. Sodium Ferulate Protects against Angiotensin II-Induced Cardiac Hypertrophy in Mice by Regulating the MAPK/ERK and JNK Pathways. *Bio. Med. Res. Int.* **2017**, *2017*, 3754942.